International Journal of Thermophysics, Vol. 20, No. 2, 1999

An Apparatus for Specific Heat Capacity Measurement by Thermal Radiation Calorimetry

K. Morimoto,[1] S. Sawai,[1] and K. Hisano[1,2]

Received May 22, 1998

Specific heat capacity measurements of disk-shaped specimens have been performed with an apparatus based on thermal radiation calorimetry. The specimen surfaces were irradiated by two flat heaters in a vacuum chamber so that homogeneous temperature distribution within an insulating specimen was achieved. Homogeneity was confirmed by computer simulation based on the control-volume method. The values of specific heat capacity were obtained by measurement of the specimen temperature, the time rate change of the specimen temperature, and the radiant power from the heater for heating and cooling modes. The specific heat capacities of Ni metal, Al_2O_3 ceramic, MgO ceramic, and AlN ceramic were measured in the temperature range from 220 to 500°C to confirm the validity of this calorimeter. The relative error involved in the measured values was estimated to be $\pm 3\%$.

KEY WORDS: calorimetry; emissivity; high temperature specific heat capacity; thermal radiation.

1. INTRODUCTION

Calorimetry based on thermal radiation heating (TRAC) has already been developed for the specific heat capacity measurement of a thin disk-shaped specimen [1]. In this calorimeter, the specimen is heated and cooled slowly by a heater in a vacuum chamber and the radiant power exchanged between the heater and the specimen is evaluated. The specimen surfaces are blackened to achieve the same emissivity for all specimens. The value of the specific heat capacity is obtained from only the specimen temperature, the radiative power of the heater, and the time rate change of the

[1] Department of Mathematics and Physics, National Defense Academy, Hashirimizu 1-10-20, Yokosuka 239-8686, Japan.

[2] To whom correspondence should be addressed.

0195-928X/99/0300-0709$16.00/0

specimen temperature in both modes. However, it was necessary to prepare thin specimens in the measurement because irradiation on one face causes an increased temperature gradient within the specimen. In fact, this type of calorimeter has also been applied to the thermal conductivity measurement of insulating materials [2, 3]. It is necessary to achieve a homogeneous distribution to obtain more reliable values of the specific heat capacity. In the present paper, an apparatus in which two flat heaters irradiate the specimen surfaces is described. The temperature gradient within a disk-shaped specimen is obtained from computer simulation based on the control-volume method for both cases of one-face and two-face irradiation [4]. The measured values of the specific heat capacity of Ni metal, Al_2O_3 ceramic, Al_2O_3 ceramic, and MgO ceramic are compared with those published in the literature.

2. THEORETICAL FORMULATION

The system in which a thin disk-shaped specimen and two flat heaters are mounted is shown schematically in Fig. 1. The specimen is heated by thermal radiation from the heaters in a vacuum chamber. The radiant power exchange between the specimen and the heaters is written as [1]:

$$MC_p \frac{dT_s}{dt} = E_h A_s (I_h - I_s) - E_s A_s (I_s - I_r) - \frac{dQ_s}{dt} \tag{1}$$

where C_p is the specific heat, M is the mass, and A_s is the surface area. T and dT/dt are the temperature and the time rate change of the specimen

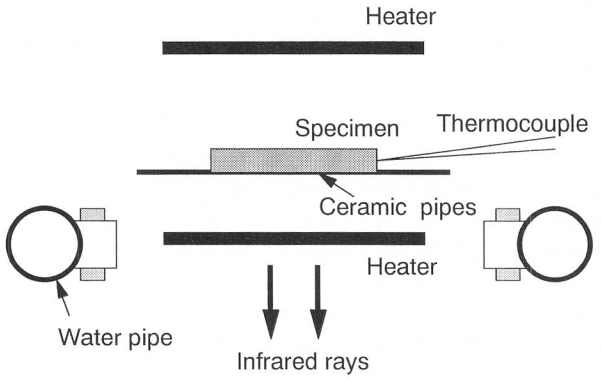

Fig. 1. Schematic setup of the heater part of the thermal radiation calorimeter. The specimen surfaces were irradiated by two flat heaters.

temperature, respectively. I is equal to σT^4, where σ is the Stefan–Boltzmann constant. Subscripts s, h, and r refer to the specimen, the heater, and the wall of the vacuum chamber, respectively. dQ_s/dt is the heat loss per unit time through thermocouple leads and ceramic pipes used to support the specimen. E_h and E_s are the "effective" emissivities expressing the radiant power exchange coefficient, which is defined in the present paper. These "effective" emissivities are constant as long as the configuration of the heaters and the specimen and the surface emissivities are the same. Equation (1) is consistent with the expression obtained from the calculation based on the net-radiation method (see the Appendix) [5, 6]. The following relation is obtained from Eq. (1) at the same specimen temperature for the heating (i) and cooling (d) modes:

$$\frac{C_p}{E_h} = \frac{A_s(I_{hi} - I_{hd})}{M(dT_{si}/dt - dT_{sd}/dt)} \tag{2}$$

The above equation implies that the value of heat capacity is obtained by evaluation of the right-hand side of the equation with the value of E_h. The heat loss term in Eq. (1) is largely canceled because of the same specimen temperature. If the heater radiant power W_h is measured by a pyrometer instead of the heater temperature T_h, we can replace I_h in Eq. (2) with W_h/G_h, where $G_h (= W_h/I_h)$ is the gain factor of the electrical circuit for the pyrometer.

The specimen surface is blackened to achieve the same high emissivity for all specimens because Eq. (1) is valid under the assumption that the reciprocity among configuration factors is satisfied. The temperature dependence of the emissivity can be estimated from the infrared emission spectrum of a rough surface blackened with high-emissivity material. The following relation gives the temperature dependence of the emissivity:

$$\varepsilon(T) = \frac{\int_0^\infty \varepsilon(\lambda)\, W(\lambda, T)\, d\lambda}{\int_0^\infty W(\lambda, T)\, d\lambda} = \frac{\int_0^\infty \varepsilon(\lambda)\, W(\lambda, T)\, d\lambda}{\sigma T^4} \tag{3}$$

where ε, $\varepsilon(\lambda)$, and $W(\lambda, T)$ are the hemispherical emissivity, the spectral emissivity, and Plank's emissive power, respectively.

3. EXPERIMENT

Figure 1 shows the schematic setup of the heater part of the calorimeter used in the present experiment. This part was set in a water-cooled vacuum chamber (20 cm in diameter and 25 cm in length) with the inside blackened with colloidal graphite. A vacuum is maintained to better than

Table I. Chemical Composition of the Ceramic Specimens

Al_2O_3 (wt%)		AlN (wt%)		MgO (wt%)	
Al_2O_3	96.6	Al	62.5	MgO	97.0
SiO_2	2.3	N	32.5	CaO	1.5
MgO	0.8	Y_2	3.4	SiO	1.5
CaO	0.3	O	1.6		

10^{-3} Pa. The specimen, supported by two alumina tubes (1 mm in diameter), was placed in the center of the two heaters made from graphite sheets (5 cm square, 0.5 mm in thickness). The heaters were separated by 2.5 cm. The heater current was controlled so that the time rate change of the specimen temperature was approximately $5°C \cdot min^{-1}$ for both heating and cooling modes. The heater radiant power W_h from the lower heater was measured by use of a pyrometer. A chromel–alumel thermocouple (0.1 mm in diameter) was placed in a hole (0.75 mm in diameter, 7 mm in depth) drilled in the side surface to measure the specimen temperature. Powder material with colloidal graphite and MnO_2 was used to blacken the heater and specimen surfaces. The emission spectrum of the material was measured by a Brucker 113v FTIR spectrometer [7]. A 99.9% pure copper specimen was used as a reference material to obtain the value of E_h at various temperatures. A specimen of 99.9% pure polycrystalline Ni metal was prepared to confirm the reliability of the present calorimeter by measuring anomalies associated with the second-order ferromagnetic phase transition. Sample materials of AlN, MgO, and Al_2O_3 ceramics synthesized by Hayashi

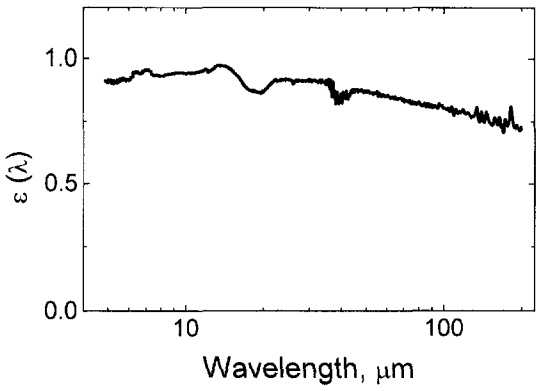

Fig. 2. Emission spectrum of the blackening material at 150°C.

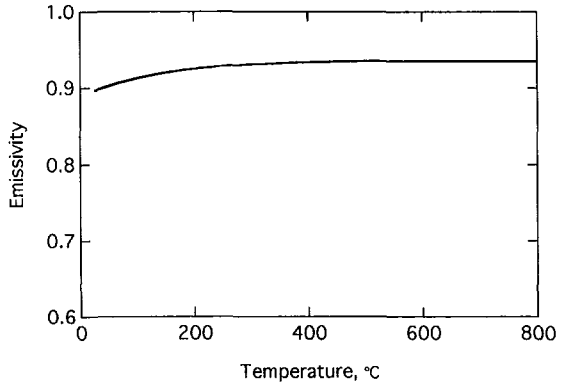

Fig. 3. Emissivity of the blackening material calculated from Eq. (4).

Chemicals (Kyoto) were also prepared. Chemical compositions of the ceramic specimens are listed in Table I. All specimens used in the present experiment have dimensions of 25 mm in diameter and 3 mm in thickness. Data for T and W_h were collected every 15 s so that an interval of about 1.25°C was obtained between data points.

4. RESULTS AND DISCUSSION

Figure 2 shows the emission spectrum if the blackening material at 150°C in the wide wavelength range from 5 to 200 μm. The emissivity is

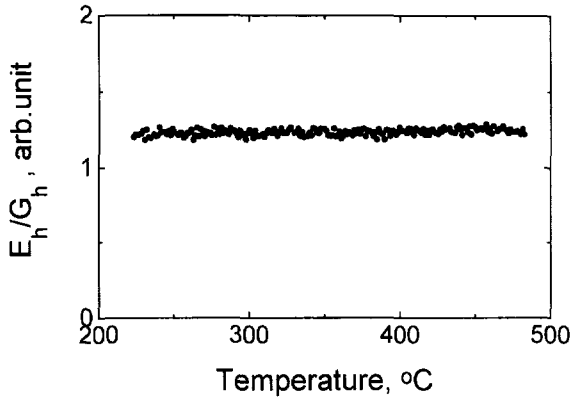

Fig. 4. Temperature dependence of E_h/G_h.

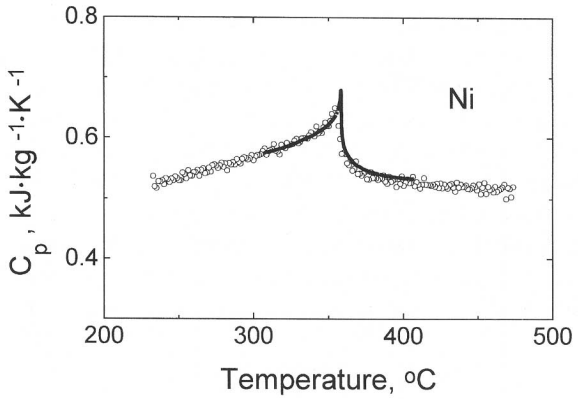

Fig. 5. Specific heat capacity of Ni specimen. The dotted line indicates the result of a single crystal specimen.

nearly 100% below 10 μm, although it decreases with increasing wavelength toward the far-infrared region. The hemispherical emissivity, ε, was calculated from the following equation because of the finite spectral range for the spectral emissivity:

$$\varepsilon(T) \approx \frac{\int_{3\,\mu\mathrm{m}}^{200\,\mu\mathrm{m}} \varepsilon(\lambda)\, W(\lambda, T)\, d\lambda}{\int_{3\,\mu\mathrm{m}}^{200\,\mu\mathrm{m}} W(\lambda, T)\, d\lambda} \tag{4}$$

The spectral emissivity from 3 to 5 μm was assumed to be the same as that at 5 μm in the calculation. As shown in Fig. 3, the emissivity becomes

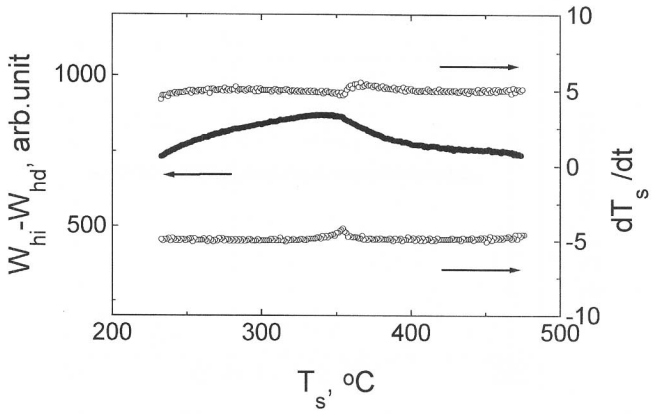

Fig. 6. Temperature dependence of $W_{hi} - W_{hd}$ and dT_s/dt of Ni specimen.

nearly constant with a value of 0.930 ± 0.02. Because the spectral emissivity of MnO_2 is higher than that of graphite in the far-infrared range, the present blackening material causes higher hemispherical emissivity than that of graphite in the lower temperature range [8]. A value of 1.26 ± 0.03 for E_h/G_h has been obtained experimentally in the temperature range from 220 to 500°C, as shown in Fig. 4. The values of the specific heat capacity of copper metal were taken from the literature [9].

Figure 5 shows the temperature dependence of the specific heat capacity of the Ni specimen showing large anomalies around the transition temperature. The dotted line indicates the result for a single crystal specimen

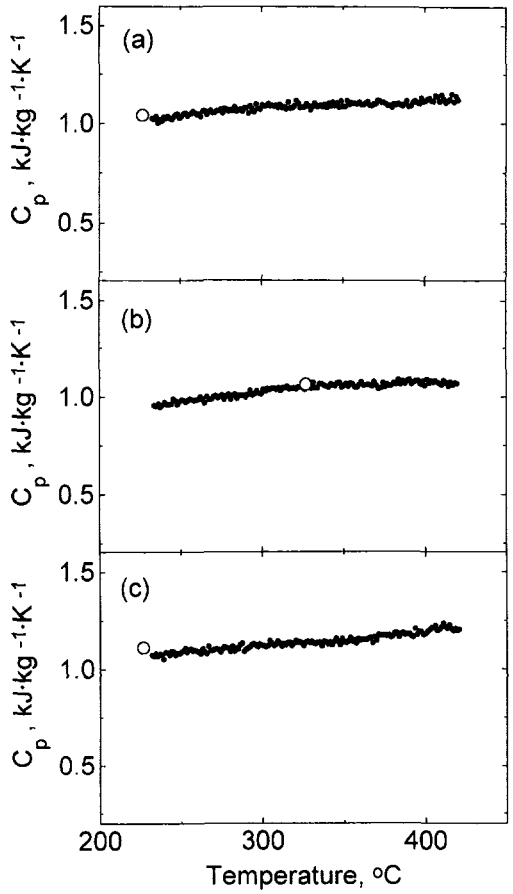

Fig. 7. Specific heat capacity of (a) Al_2O_3, (b) AlN, and (c) MgO ceramics. The open circles show the recommended values.

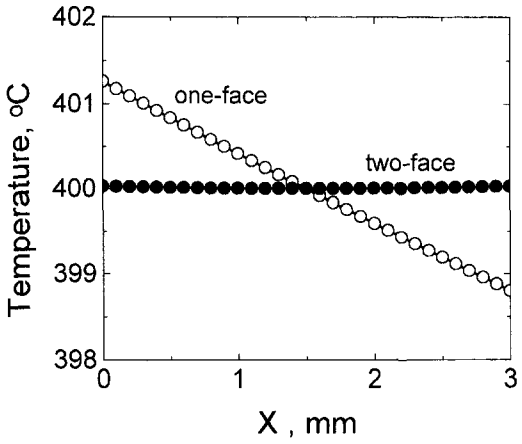

Fig. 8. Temperature distribution within Al_2O_3 for the cases of one-face and two-face irradiation obtained from the calculation based on the control-volume method.

obtained by previous authors [10]. No anomaly caused by the latent heat was included in the temperature dependence because of the second-order phase transition. The anomalies are also observed in the temperature dependence of $W_{hi} - W_{hd}$ and dT_s/dt as shown in Fig. 6. The deviation from the result of the single crystal is about $\pm 3\%$ around 350°C.

Figure 7 shows, respectively, tile specific heat capacities of (a) Al_2O_3, (b) AlN, and (c) MgO ceramics obtained in the present experiment. The open circles indicate the recommended values [11, 12].

Figure 8 shows the temperature distribution within the Al_2O_3 specimen for a heating mode with a rate change of $5°C \cdot min^{-1}$. The results for both cases of one-face and two-face irradiation were obtained from the calculation based on the control-volume method [4]. The values of thermophysical properties needed for the calculations were taken from the literature [11, 12]. The two-face irradiation achieves a homogeneity within 0.2°C. The relative error involved in the values estimated from Eq. (2) is about $\pm 3\%$ in the present measurements.

5. CONCLUSION

Measurement of the specific heat capacity of disk-shaped specimens has been performed with an apparatus based on the TRAC. Both specimen surfaces were irradiated by two flat heaters so that a homogeneous temperature distribution within the specimen was achieved in the present experiment,

unlike the case of one-face irradiation. The values of the specific heat capacity were obtained at various temperatures by use of a simple theoretical formulation. The relative error involved in the measured values was estimated to be $\pm 3\%$.

APPENDIX

The net-radiation method is applied to an enclosure composed of gray surface. The following two basic relations are considered for an enclosure composed of N discrete surface areas

$$Q_k = A_k \frac{\varepsilon_k}{1-\varepsilon_k}(\sigma T_k^4 - q_{o,k}) \tag{A1}$$

$$Q_k = A_k \left(q_{o,k} - \sum_{j=1}^{N} F_{k-j} q_{o,j} \right) \tag{A2}$$

where Q_k is the power supplied to the surface k by external means. F_{k-j} is the configuration factor which defines the fraction of radiant power leaving the surface k that arrives at the surface $j \cdot q_{o,k}$ is the radiant power per unit area leaving the surface k. The reciprocal relation among the configuration factors is assumed to be held in the method. That is given as

$$A_k F_{k-j} = A_j F_{j-k} \tag{A3}$$

Let us derive the expression for radiation exchange among the specimen and heaters for the system in Fig. A1. The enclosure consists of the specimen surface, the heater surfaces, and the cylindrical side surface, which is assumed to be a perfect absorber. The following relations are obtained from Eq. (A2):

$$\begin{aligned}
\frac{Q_s}{A_s} &= q_s = q_{o,s} - F_{s-1} q_{o,1} - F_{s-2} q_{o,2} - F_{s-3} q_{o,3} \\
\frac{Q_1}{A_1} &= q_1 = q_{o,1} - F_{1-2} q_{o,2} - F_{1-3} q_{o,3} - F_{1-s} q_{o,s} \\
\frac{Q_2}{A_2} &= q_2 = q_{o,2} - F_{2-1} q_{o,1} - F_{2-3} q_{o,3} - F_{2-s} q_{o,s} \\
\frac{Q_3}{A_3} &= q_3 = q_{o,3} = I_3
\end{aligned} \tag{A4}$$

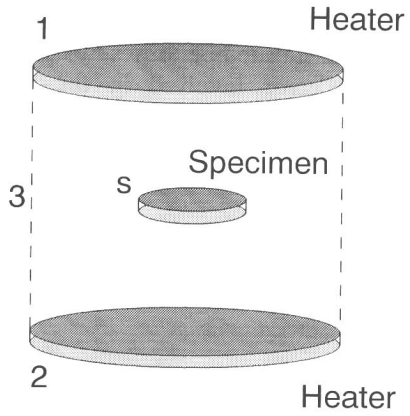

Fig. A1. The enclosure composed of the specimen surface, the heater surfaces, and the cylindrical side surface.

where subscripts s, 1, 2, and 3 indicate the specimen, the upper heater, the lower heater, and the side surfaces, respectively. Equation (A1) is used to derive the following relations for the present system:

$$\begin{aligned} q_{\mathrm{o,s}} &= I_{\mathrm{s}} - \frac{\rho}{\varepsilon} q_{\mathrm{s}} \\ q_{\mathrm{o,1}} &= I_1 - \frac{\rho}{\varepsilon} q_1 \\ q_{\mathrm{o,2}} &= I_2 - \frac{\rho}{\varepsilon} q_2 \\ q_{\mathrm{o,3}} &= I_3 \end{aligned} \tag{A5}$$

where ρ is the reflectivity. The relation $\rho = 1 - \varepsilon$ must be valid for the opaque gray surfaces. We find the following expression for q_{s} by substituting Eq. (A5) into Eq. (A4):

$$\begin{aligned} q_{\mathrm{s}} = \frac{1}{D} \{ &(I_{\mathrm{s}} - I_1)(XF_{\mathrm{s-1}} - Y + ZF_{\mathrm{2-1}}) + (I_{\mathrm{s}} - I_2)(XF_{\mathrm{s-2}} + YF_{\mathrm{1-2}} - Z) \\ &+ (I_{\mathrm{s}} - I_3)(XF_{\mathrm{s-3}} + YF_{\mathrm{1-3}} - ZF_{\mathrm{2-3}}) \} \end{aligned} \tag{A6}$$

where D, X, Y, and Z are given as

$$D = \begin{vmatrix} \eta+1 & -\eta F_{s-1} & -\eta F_{s-2} \\ -\eta F_{1-s} & \eta+1 & -\eta F_{1-2} \\ -\eta F_{2-s} & -\eta F_{2-1} & \eta+1 \end{vmatrix}$$

$$X = (\eta+1)^2 - \eta F_{1-2} F_{2-1} \tag{A7}$$

$$Y = \eta(\eta+1) F_{s-1} - \eta^2 F_{s-2} F_{2-1}$$

$$Z = \eta^2 F_{1-2} F_{s-1} + \eta(\eta+1) F_{s-2}$$

where $\eta = \rho/\varepsilon$. If I_1 and I_2 are I_h, moreover, if I_3 is I_r, we obtain the expression for the energy exchange in the present system. That is,

$$q_s = E_h(I_s - I_h) - E_s A_s(I_s - I_r) \tag{A8}$$

q_s is the power supplied to the specimen surface by the change of specimen heat capacity. Therefore, the following relation is obtained:

$$\frac{C_p M}{A_s}\frac{dT_s}{dt} = E_h(I_h - I_s) - E_s(I_s - I_r) \tag{A9}$$

E_h and E_s are functions of the emissivity, and the configuration factors are constant as long as these quantities are constant. The expression for E_h and E_s is much too complicated to cite. The expression as Eq. (A8) can be adapted to the square heater system used in the present experiment although the calculation was made for the circular heater system.

REFERENCES

1. K. Hisano and T. Yamamoto, *High Vend. High Press.* **25**:337 (1993).
2. K. Hisano and F. Placido, *High Temp. High Press.* **30**:287 (1997).
3. K. Hisano, S. Sawai, and K. Morimoto, *Int. J. Thermophys.* **19**:291 (1998).
4. P. J. Roache, *Computational Fluid Dynamic* (Hermosa, Albuquerque, 1976).
5. H. C. Hottel and A. F. Sarofim, *Radiative Transfer* (McGraw-Hill, New York, 1972).
6. R. Siegel and J. R. Howell, *Thermal Radiation Heat Transfer* (McGraw-Hill, New York, 1972).
7. A. Aoki, H. Tanaka, and K. Hisano, in *Proc. 12th Japan Symp. Thermophys. Prop.*, Vol. 12 (Japan. Soc. Thermophys. Prop., Kyoto, 1991), p. 9.
8. K. Hisano, S. Sawai, and K. Morimoto, *Int. J. Thermophys.* **19**:305 (1998).
9. D. E. Gray (ed.) *American Institute of Physics Handbook* (McGraw-Hill, New York, 1972).
10. D. L. Connelly, J. S. Loomis, and D. E. Mapother, *Phys. Rev. B* **3**:924 (1971).
11. Y. S. Touloukian and E. H. Buyco, *Thermophysical Properties of Matter, 5. Nonmetallic Solids, Specific Heat* (Plenum, New York, 1970).
12. Y. S. Touloukian, *Thermophysical Properties of Matter, 2. Nonmetallic Solids, Thermal Conductivity* (Plenum, New York, 1970).